AGU PUBLICATIONS

GeoHealth

RESEARCH ARTICLE
10.1002/2017GH000089

Key Points:
- Climate change may cause increases in season length and spatial habitat for *V. vulnificus* and *V. parahaemolyticus* in the Chesapeake Bay
- Increase in favorable habitat for *V. cholerae* was less marked and restricted to low salinity regions of the Bay

Supporting Information:
- Supporting Information S1

Correspondence to:
B. A. Muhling,
barbara.muhling@noaa.gov

Citation:
Muhling, B. A., J. Jacobs, C. A. Stock, C. F. Gaitan, and V. S. Saba (2017), Projections of the future occurrence, distribution, and seasonality of three *Vibrio* species in the Chesapeake Bay under a high-emission climate change scenario, *GeoHealth*, *1*, 278–296, doi:10.1002/2017GH000089.

Received 28 APR 2017
Accepted 4 AUG 2017
Published online 26 SEP 2017

This article was corrected on 15 JUL 2019. The online version of this article has been modified to include a Conflict of Interest statement.

Projections of the future occurrence, distribution, and seasonality of three *Vibrio* species in the Chesapeake Bay under a high-emission climate change scenario

Barbara A. Muhling[1,2,3], John Jacobs[4], Charles A. Stock[2], Carlos F. Gaitan[5], and Vincent S. Saba[6]

[1]Princeton University Program in Atmospheric and Oceanic Sciences, Princeton, New Jersey, USA, [2]NOAA Geophysical Fluid Dynamics Laboratory, Princeton, New Jersey, USA, [3]Now at Cooperative Institute for Marine Ecosystems and Climate, University of California, Santa Cruz, California, USA, [4]National Oceanic and Atmospheric Administration, National Ocean Service, National Centers for Coastal Ocean Science, Cooperative Oxford Lab, Oxford, Maryland, USA, [5]Arable Labs Inc., Princeton, New Jersey, USA, [6]National Oceanic and Atmospheric Administration, National Marine Fisheries Service, Northeast Fisheries Science Center, Geophysical Fluid Dynamics Laboratory, Princeton University Forrestal Campus, Princeton, New Jersey, USA

Abstract Illness caused by pathogenic strains of *Vibrio* bacteria incurs significant economic and health care costs in many areas around the world. In the Chesapeake Bay, the two most problematic species are *V. vulnificus* and *V. parahaemolyticus*, which cause infection both from exposure to contaminated water and consumption of contaminated seafood. We used existing *Vibrio* habitat models, four global climate models, and a recently developed statistical downscaling framework to project the spatiotemporal probability of occurrence of *V. vulnificus* and *V. cholerae* in the estuarine environment, and the mean concentration of *V. parahaemolyticus* in oysters in the Chesapeake Bay by the end of the 21st century. Results showed substantial future increases in season length and spatial habitat for *V. vulnificus* and *V. parahaemolyticus*, while projected increase in *V. cholerae* habitat was less marked and more spatially heterogeneous. Our findings underscore the need for spatially variable inputs into models of climate impacts on *Vibrios* in estuarine environments. Overall, economic costs associated with *Vibrios* in the Chesapeake Bay, such as incidence of illness and management measures on the shellfish industry, may increase under climate change, with implications for recreational and commercial uses of the ecosystem.

Plain Language Summary Bacteria in the genus *Vibrio* can cause illness to people through eating of contaminated seafood, or exposure to contaminated water. *Vibrios* occur naturally in the Chesapeake Bay, but their abundance varies with water temperature, salinity and other factors. We assessed the potential effects of climate change on the future abundance of three *Vibrios* in the Chesapeake Bay using outputs from four different climate models. We show that abundance of *Vibrios* in the water, and in oysters, may increase as temperatures warm. In addition, the seasons of highest risk may last longer, compared to the present day. This suggests that *Vibrio*-related illnesses in the Chesapeake Bay region may increase in the future, unless current management measures can adapt.

1. Introduction

Many species of bacteria in the genus *Vibrio* are pathogenic to humans [*Farmer et al*., 2005]. Globally, the most well known is *V. cholerae*, the causative agent for cholera [*Waldman et al*., 2013]. There are estimated to be more than 1 million cases of cholera worldwide each year, with thousands of associated deaths [*World Health Organization*, 2016]. However, other *Vibrio* species also cause serious illness through consumption of contaminated seafood and environmental exposure.

In the United States, the two most problematic are *V. parahaemolyticus* and *V. vulnificus*, with other species including *V. cholerae* (nonepidemic strains) and *V. alginolyticus* also contributing to *Vibrio*-associated illnesses [*Ralston et al*., 2011; *Jones et al*., 2013]. It is estimated that there are more than 34,000 cases of *V. parahaemolyticus* infection each year, with about $40 million in associated economic costs. *V. vulnificus* infections are much rarer but are more likely to lead to hospitalization and serious illness, with mortality rates of 30–40%

[*Ralston et al*., 2011; *Scallan et al*., 2011; *Hoffmann et al*., 2015]. As a result, although there are only around 200–300 cases each year, these are associated with around $320 million in economic costs, including medical services, lost wages, and cost of premature death. *V. parahaemolyticus* is primarily transmitted through contaminated seafood, while *V. vulnificus* infections result from both foodborne sources and direct recreational exposure [e.g., from swimming with open wounds, *Ralston et al*., 2011].

Recent studies have suggested that the incidence of *Vibrio* infections may be increasing in some coastal oceans in association with warming temperatures [*Andersson and Ekdahl*, 2006; *Martinez-Urtaza et al*., 2010; *Vezzulli et al*., 2010a, 2016; *Le Roux et al*., 2015]. Several have highlighted correlations between *Vibrio* outbreaks and anomalously warm conditions [*Paz et al*., 2007; *Baker-Austin et al*., 2013, 2017]. Heat waves have been associated with the occurrence of new strains of *Vibrio* to a region [*Martinez-Urtaza et al*., 2013] and to the outbreak of *Vibrio*-related disease in areas where this was previously rare or unknown [*Baker-Austin et al*., 2017]. Due to the seriousness of *Vibrio*-related illnesses, the potential for increased incidence of infections in warming waters under climate change has significant economic and social implications [*Lipp et al*., 2002; *Martinez-Urtaza et al*., 2010; *Jacobs et al*., 2015]. Laboratory experiments have shown optimum temperatures for several *Vibrio* species of 37–39°C, which is much warmer than currently observed water temperatures in the estuarine and marine environments where *Vibrios* are found [*Kelly*, 1982; *Miles et al*., 1997; *Sedas*, 2007]. In addition, current seasonal occurrences of *Vibrios* appear to be restricted by winter water temperatures. For example, in the southern states bordering the Gulf of Mexico, *V. vulnificus* has been recorded in coastal and estuarine waters year round [*Lipp et al*., 2001], and *Vibrio*-associated illnesses are recorded in all months of the year [*Altekruse et al*., 2000]. In contrast, *Vibrio* occurrence is generally restricted to the warmest months of the year in higher latitudes of the mid-Atlantic and New England [*O'Neill et al*., 1992; *Jacobs et al*., 2014]. Warming waters may therefore extend the length of high-risk seasons for *Vibrio*-related illnesses in regions where they are already known to occur, as well as facilitating their introduction to new areas [e.g., *Baker-Austin et al*., 2013; *Vezzulli et al*., 2016]. However, there are relatively few studies which use projections from Intergovernmental Panel on Climate Change (IPCC) climate models to examine the risk of future *Vibrio* species occurrence or rates of infection.

Several *Vibrio* species occur naturally in the Chesapeake Bay, including *V. cholerae*, *V. parahaemolyticus*, and *V. vulnificus* [*Colwell et al*., 1977; *Wright et al*., 1996]. All three show positive relationships with water temperature and occur more frequently and at higher abundances over the warmer months [*Kaneko and Colwell*, 1973; *Louis et al*., 2003; *Jacobs et al*., 2010]. This is consistent with published relationships from other areas around the world, where *Vibrios* are rarely collected in waters cooler than 10–15°C and tend to increase in abundance when temperatures exceed about 20°C [*O'Neill et al*., 1992; *Kaspar and Tamplin*, 1993; *Randa et al*., 2004; *McLaughlin et al*., 2005; *Vezzulli et al*., 2010a, 2013; *Baker-Austin et al*., 2010, 2013; *Turner et al*., 2014; *Haley et al*., 2014]. In contrast, each *Vibrio* species appears to be associated with a distinct, species-specific salinity range. *V. parahaemolyticus* has the widest range, from approximately 5 to 30 (practical salinity unit, psu) [*United States Food and Drug Administration* (*USFDA*), 2005; *Parveen et al*., 2008], while *V. vulnificus* occurs from near-fresh salinities to approximately 24 psu but is most common at around 8–16 [*Jacobs et al*., 2014]. These observations are consistent with the salinity tolerances reported elsewhere for these species [*Kelly*, 1982; *Kaspar and Tamplin*, 1993; *Lipp et al*., 2001; *Pfeffer et al*., 2003; *Randa et al*., 2004; *Martinez-Urtaza et al*., 2010]. In contrast, *V. cholerae* occurs most frequently in the Chesapeake Bay where salinity is low (less than 8 psu) [*Louis et al*., 2003]. As these authors note, this relationship is not consistent among regions, as *V. cholerae* has been found from near fresh to moderately high (greater than 20 psu) salinities in other locations [*Huq et al*., 1984; *Jiang and Fu*, 2001; *Louis et al*., 2003; *Chávez et al*., 2005]. This likely reflects the strong dependence of *V. cholerae* on other environmental variables which are correlated with salinity, such as nutrients or concentration of zooplankton species [*Louis et al*., 2003; *Baker-Austin et al*., 2010; *Vezzulli et al*., 2010b, 2016; *Constantin de Magny et al*., 2011]. Overall, current data suggest that climate change may lead to increasing numbers of *Vibrios*, and potentially of *Vibrio*-related illnesses in the Chesapeake Bay, but only in those regions of the Bay where other environmental conditions remain (or become) favorable.

Jacobs et al. [2015] addressed aspects of this question by applying predictive models for *V. parahaemolyticus* and *V. vulnificus* to projections of future water temperature from downscaled global climate models. They used near-surface air temperature as a proxy for surface water temperature, based on historical relationships from observations. Multiple sites along the United States coast were examined, including the Chesapeake

Table 1. Logistic Generalized Linear Models for Three *Vibrio* Species (*V. vulnificus*, *V. cholerae*, and *V. parahaemolyticus*)[a]

Species	Equation	Source
V. vulnificus	Logit [Vv] = 0.211*SST − 0.272*SALOPT − 4.288 ProbPres = $e^{logit}/[1 + e^{logit}]$	*Jacobs et al.* [2014]
V. cholerae	Logit [Vc] = 0.1233*SST − 0.1997*SSS − 0.0324*SST*SSS ProbPres = $e^{logit}/[1 + e^{logit}]$	*Louis et al.* [2003]
V. parahaemolyticus	log[Vp/g] = − 2.05 + 0.097*SST + 0.2*SSS − 0.0055*SSS^2	*USFDA* [2005]

[a]SST refers to surface water temperature, while SSS is surface salinity (psu). SALOPT refers to the absolute distance of measured salinity from 11.5, the optimal salinity for this species [*Jacobs et al.*, 2014].

Bay. These authors found that increasing temperatures would likely lead to expanded seasons of occurrence for both species. However, an important aspect of *Vibrio* risk assessment is the spatial location of high-risk areas [e.g., *Constantin De Magny et al.*, 2009; *Jacobs et al.*, 2010; *Banakar et al.*, 2011]. The narrower salinity range favored by *V. cholerae* and *V. vulnificus*, in particular, results in spatially localized "hot spots," which shift according to streamflow and salinity conditions. Future precipitation patterns under climate change are uncertain for the Chesapeake Bay region [*Najjar et al.*, 2010]. Some climate models project strong increases in freshwater inflow, which would move high-risk areas downriver in tributaries and down bay (seawards) in the main stem. Other models project minimal change in watershed precipitation, which when added to warming watershed temperatures and increased evapotranspiration may result in increased salinity in most locations in the Bay [*Muhling et al.*, 2017]. Under these conditions, high-risk *Vibrio* areas may move upstream. Spatial projections of temperature and salinity in the Chesapeake Bay are thus required to more fully assess changes in the location of high-risk *Vibrio* hot spots.

In this study, we used a recently developed statistical downscaling and spatial disaggregation modeling framework for estuarine habitats [*Muhling et al.*, 2017] to project future spatial distribution and season length for three *Vibrio* species in the Chesapeake Bay, using general circulation models (GCMS) run under a high-emission climate change scenario. We used previously published regression models to predict probability of occurrence or concentration for each species within eight regions of the Chesapeake Bay. The ability of the framework to capture habitat variability within each subregion, to the extent required to differentiate years with low versus high probability of occurrence or concentration, was assessed for each species.

2. Methodology

2.1. Habitat Models

Suitable habitat for occurrence of *V. cholerae* and *V. vulnificus* was predicted using the multivariate logistic generalized linear models (GLMs) published by *Louis et al.* [2003] and *Jacobs et al.* [2014], respectively. In addition, the concentration of *V. parahaemolyticus* in oysters (*Crassostrea virginica*) in $\log_{10}$ colony forming units (CFU)/gram was predicted using the relationships reported by the U.S. Food and Drug Administration [*USFDA*, 2005]. All models used surface temperature and surface salinity as predictor variables (Table 1). Models for *Vibrio* species were applied to the entire Chesapeake Bay main stem and major tributaries (Figure 1).

Sampling for *V. vulnificus* took place in January, April, July, and October 2007, and April, July, and October 2008–2010 [*Jacobs et al.*, 2014]. Surface (0.5 m depth) water samples were collected from the main stem and major tributaries of the Chesapeake Bay, stored in sterile polypropylene bottles, and then frozen until sampling was completed for the month. After thawing, samples were filtered, and the filtered material was tested for *V. vulnificus* using quantitative Polymerase Chain Reaction (qPCR). While *Jacobs et al.* [2014] also determined abundance (CFU/mL), we only considered the probability of occurrence (presence/absence) for *V. vulnificus* in this study (Table 1). This GLM showed 86.6% agreement between modeled and observed probabilities of occurrence for *V. vulnificus*, with an Area Under the Receiver Operating Curve (AUC) of 0.87 [*Jacobs et al.*, 2014].

Sampling for *V. cholerae* was completed at least monthly between January 1998 and February 2000 at nearshore sites in the upper Chesapeake Bay, and during summer 1999 and 2000 in the main stem [*Louis et al.*, 2003]. Both water and plankton samples were collected, and *V. cholerae* was isolated using the alkaline peptone water-enrichment procedure. Presumptive *V. cholerae* isolates were confirmed by PCR [*Louis et al.*, 2003]. The GLM showed 76.9% agreement between observations and modeled probabilities of occurrence. Both

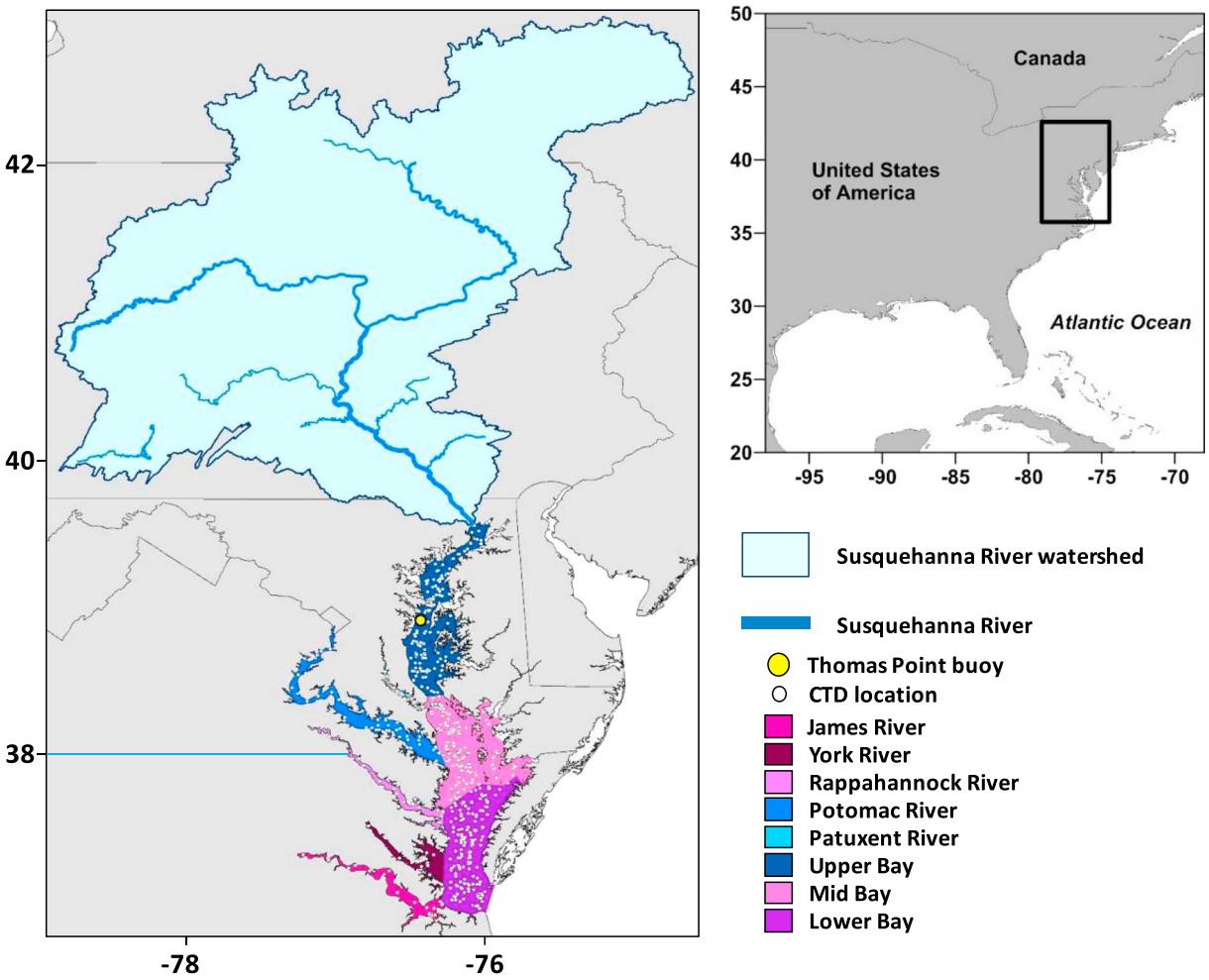

Figure 1. Study area showing the Susquehanna River watershed, the location of the Thomas Point buoy, and the Chesapeake Bay and major tributaries. CTD cast stations used to develop the statistical framework (Figure 3) are also shown. Colors denote the eight zones of the Bay mentioned in the text.

temperature and salinity were statistically significant within the model ($p < 0.05$), as was an interaction between the two [*Louis et al*., 2003] (Table 1).

The United States Food and Drug Administration (USFDA) model for *V. parahaemolyticus* densities in oysters was developed using data from multiple studies conducted across the United States, including the Pacific, Atlantic, and Gulf of Mexico coasts. Temperature and salinity were obtained in situ where possible, and the GLM estimating *V. parahaemolyticus* in oysters was parameterized using the Tobit regression method [*USFDA*, 2005]. This study notes that water temperature explained approximately 50% of the variance in (log) *V. parahaemolyticus* concentrations, but no information on the overall skill of the model was given. However, both temperature and salinity were highly significant within the GLM ($p < 0.0001$) (Table 1).

Applying each *Vibrio* habitat model from Table 1 across two-dimensional temperature/salinity space illustrates the differences in habitat preferences across species (Figure 2).

Strong differences between *V. cholerae* and the other species are particularly evident. All three *Vibrios* had higher probability of occurrence at warmer temperatures, while *V. vulnificus* and *V. parahaemolyticus* were predicted to be most abundant at moderate salinities, and *V. cholerae* was associated with low salinity (less than 8 psu). The *V. vulnificus* and *V. parahaemolyticus* models suggested that these species occurred across a wider range of salinities when temperatures were very warm. Optimum salinity values stretched across a fairly broad range (8–16 psu) for *V. vulnificus* and an even larger range (5–30 psu) for *V. parahaemolyticus*.

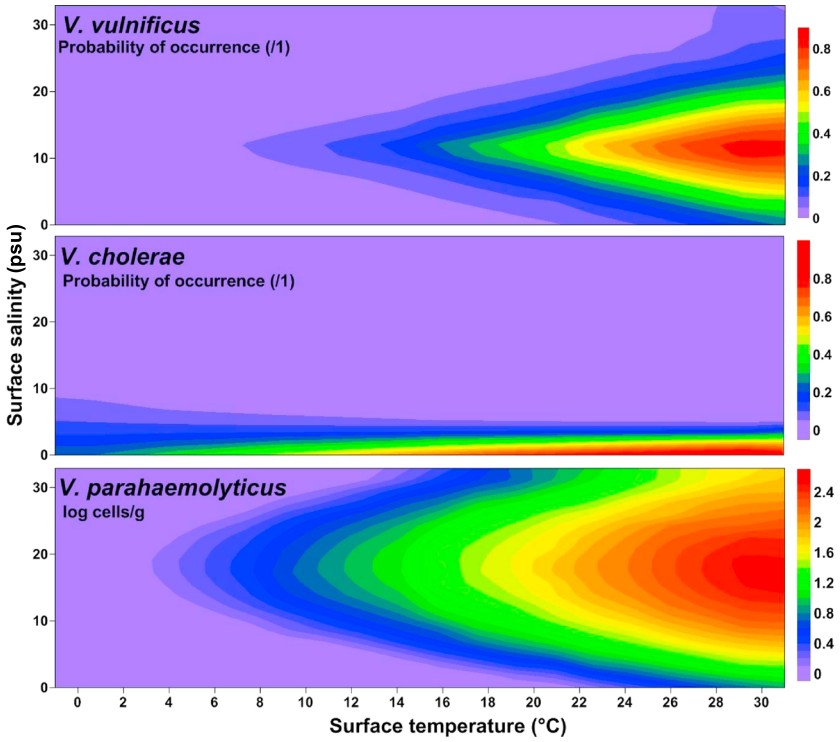

Figure 2. Representation of the GLMs in Table 1 in temperature-salinity two-dimensional space for *V. vulnificus*, *V. cholerae*, and *V. parahaemolyticus*.

2.2. Habitat Projection Framework

Historical estimates and future projections of surface temperature and salinity across the Chesapeake Bay were sourced from a previously published statistical downscaling framework [*Muhling et al*., 2017: Figure 3]. A brief summary of the framework follows, and the reader is directed to *Muhling et al*. [2017] for further details.

The framework ingests air temperature at the Thomas Point buoy and air temperature/precipitation over the Susquehanna River watershed and uses a hierarchy of models to estimate spatial fields of surface temperature and salinity across the Chesapeake Bay. For future projections, the inputs to the framework are statistically downscaled air temperature and precipitation from GCMs (see section 2.3 "Future Projections" below for details). For historical estimates, inputs are observed air temperature at Thomas Point, and precipitation and air temperature in the Susquehanna River watershed from the NOAA/National Centers for Environmental Prediction GHCN (Global Historical Climatology Network) Climate Anomaly Monitoring System (CAMS) 0.5° monthly temperature data set [*Fan and van den Dool*, 2008], and the CPC (Climate Prediction Center) Unified Gauge-Based 0.25° Analysis of Daily Precipitation (CPC) [*Chen et al*., 2008].

Streamflow is derived from downscaled air temperature and precipitation over the Susquehanna River basin using a simple water balance model [*McCabe and Markstrom*, 2007], calibrated for Chesapeake Bay as described in *Muhling et al*. [2017]. Comparison of predicted versus observed monthly Susquehanna River streamflow at Conowingo dam from 1970 to 2006 showed that the model reproduced observations with good skill (R^2 = 0.8 [*Muhling et al*., 2017]).

Spatial estimates of surface temperature and salinity were estimated from air temperature and streamflow anomalies using linear model trees [*Quinlan*, 1992] with the Cubist package in R 3.2.1 [*Kuhn et al*., 2015; *R Core Team*, 2015]. Linear model trees are similar to regression trees, but the predicted values at terminal nodes are described using multivariate linear equations rather than fixed values. This characteristic allows model trees to extrapolate beyond the range of training data, whereas many other machine-learning techniques cannot [*Quinlan*, 1992, 1993]. The predictor variables are used both to split the training data into increasingly similar subsets and to parameterize the equations at the terminal nodes.

Models were trained on conductivity-temperature-depth (CTD) cast data from the Chesapeake Bay Program, the University of Maryland Chesapeake Biological Laboratory cruise database, and the Smithsonian Environmental Research Center database from 1986 to 2005 and then validated with out-of-sample data from the same programs from 2006 to 2015 [*Muhling et al*., 2017]. Surface temperature was predicted using 17 day moving mean air temperatures at Thomas Point, the 30 day change in this metric (to account for seasonal hysteresis [*Letcher et al*., 2016]), freshwater inflow at Conowingo Dam, time of day, latitude, and longitude. Surface salinity was predicted using the same variables, except that Thomas Point air temperature was not included.

Previous validation of temperature and salinity anomalies across the regions identified in Figure 1 showed robust out-of-model temperature anomaly prediction skill across regions (R^2 between 0.62 and 0.77) and considerable skill for surface salinity (R^2 between 0.42 and 0.76 [*Muhling et al*., 2017]). The translation of these hydrographic skill metrics to accurate prediction of *Vibrio* habitat favorability, however, is less clear. Before making projections, we thus assessed whether out-of-sample estuarine *Vibrio* habitat estimates derived from our downscaling framework were consistent with those derived from the CTD data. That is, are *Vibrio* habitat projections based on statistically downscaled and spatially disaggregated habitat estimates of comparable accuracy to those based on real-time hydrographic observations? We assessed skill for the regions defined in Figure 1 and at the subregional scale across individual CTD casts.

2.3. Future Projections

To assess the potential impacts of climate change on the occurrence of *Vibrio* species in the Chesapeake Bay, we used statistically downscaled projections under RCP8.5 from four GCMs with contrasting characteristics for the region, spanning the range of future warming and precipitation projections [*Muhling et al*., 2017]. RCP8.5 is a high-emission scenario, which assumes that radiative forcing due to greenhouse gas emission will continue to increase strongly throughout the 21st century [*Riahi et al*., 2011]. The GFDL-CM3 model (hereafter CM3 model) [*Donner et al*., 2011] showed strong warming of the surface air temperature (an increase of around 5.0–5.5°C) between historical (1970–1999) and end of century (2071–2100) periods under RCP8.5, and a mean annual increase in precipitation over the Susquehanna River watershed of approximately 0.75 mm/d. The MRI-CGCM-3 model (hereafter MRI model) [*Yukimoto et al*., 2012] showed a slightly lower precipitation increase (around 0.5 mm/d on average) and much weaker warming of around 2.0–2.5°C by the end of the century. The IPSL-CM5A-LR model (hereafter IPSL model) [*Dufresne et al*., 2013] warmed around 4.5–5.0°C between the historical and end century time periods but showed little change in mean precipitation over the region. The GFDL-ESM2G model (hereafter ESM2G) [*Dunne et al*., 2012] showed a slight precipitation increase (around 0.2 mm/d) and weaker warming of around 3.0–3.5°C by the end of the century. The CM3 model thus represented a warmer, wetter future, the MRI model a less warm, wetter future, the IPSL model a warmer, precipitation-neutral scenario, and the ESM2G model a less warm, precipitation-neutral future.

Each of the four GCMs was bias corrected using four separate statistical methods—Bias-Corrected Quantile Mapping, Change Factor Quantile Mapping, Equidistant Quantile Mapping, and the Cumulative Distribution Function Transform—and then spatially disaggregated using linear model trees. Results from *Muhling et al*. [2017] showed that projections using the different downscaling methods were similar except at extreme high temperatures, and that choice of downscaling method was much less influential than choice of GCM for our application. We therefore averaged projections from each GCM across all four downscaling methods and present results only among different GCMs.

The CPC daily precipitation analysis was used as the historical observations for the Susquehanna River watershed, by assigning each grid point from this 0.25 × 0.25° resolution analysis (n = 119, 1970–2005) to the closest grid point for each GCM (n = 2–6). Watershed air temperature observations for downscaling were obtained from eight weather stations (1970–2005) and then also assigned to the closest grid point for each GCM. Air temperatures at Thomas Point were obtained from only one grid point from each GCM and were downscaled using historical observed air temperatures at the Thomas Point buoy (1985–2015). Downscaled air temperature and precipitation fields were then run through the modeling framework (Figure 3) to obtain surface temperature and salinity fields in the Chesapeake Bay for the recent historical (1970–1999) and end century future (2071–2100) time periods, for each GCM [*Muhling et al*., 2017]. The *Vibrio* models in Table 1 were then applied to these fields and used to compare potential changes in probability of occurrence of

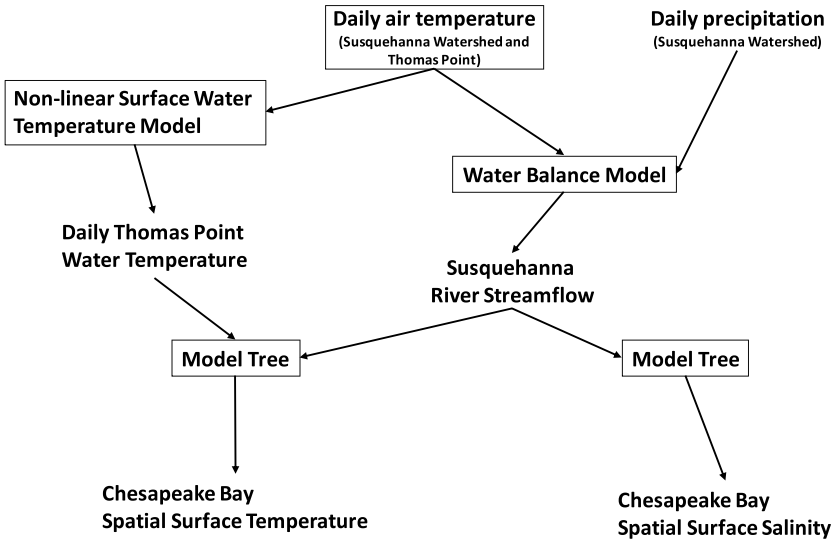

Figure 3. Schematic representation of the statistical framework developed by *Muhling et al.* [2017]. Models are boxed, and model outputs are unboxed. Adapted with permission of Springer, from Estuaries and Coasts doi: 10.1007/s12237-017-0280-8, 2017.

V. vulnificus and *V. cholerae*, and the concentration of *V. parahaemolyticus* in oysters, between the two time periods.

3. Results

The mean habitat favorability predicted from observed temperature and salinity was similar to that predicted using out-of-sample temperature and salinity estimates derived from the statistical downscaling framework (Figure 4, bars). While the framework introduced some error into predictions from the *Vibrio* habitat models when compared to CTD observations, this was generally minimal (e.g., probabilities of occurrence by zone (Figure 1) differed by less than 5% for both *V. vulnificus* and V. *cholerae*). The R^2 values derived between CTD-based and downscaled estuarine conditions within each zone of the Chesapeake Bay during peak seasons were above 0.6 for all species and zones, except for *V. cholera* within higher salinity environments where the probability of occurrence is very low (Figure 4, value above bars). In these regions, minimally varying probabilities of occurrence near zero resulted in low R^2 values.

Consistent with the relationships shown in Figure 2, *V. cholerae* was predicted to be most prevalent in lower salinity environments (upper reaches of the James, Potomac, and Rappahannock Rivers and Upper Bay). *V. vulnificus* had the highest probabilities of occurrence in moderate salinity zones (Mid Bay, Patuxent and Rappahannock Rivers, and Upper Bay), while *V. parahaemolyticus* was abundant across most of the bay except the Potomac River (Figure 4).

Application of habitat models to future projections from downscaled GCMs resulted in higher mean monthly probability of occurrence for *V. vulnificus* (Figure 5, top panel) between April and October. This difference was strongest in the warmer CM3 and IPSL models and weakest in the MRI model. In contrast, probabilities of occurrence for *V. cholerae* (Figure 5, middle) increased substantially in winter-spring in the warmer, wetter CM3 model, increased slightly in the MRI model, and decreased in the drier IPSL model. Probabilities of occurrence for *V. cholerae* between June and November were not projected to change strongly. Mean CFU/g of *V. parahaemolyticus* in oysters (Figure 5, bottom) was predicted to increase at all times of year, particularly in summer and fall. Increases were strongest in the warmer CM3 and IPSL models, and weaker in the MRI model.

To show the range of possible future changes in spatial habitat, we selected the two most divergent GCMs for each *Vibrio* species from Figure 5 and focus on seasons of peak occurrence. For *V. vulnificus* these were the CM3 (most warming) and MRI (least warming) models (Figure 6). Projections suggested an overall increase in probability of occurrence across the Chesapeake Bay in summer by the end of the century. This increase was much stronger in the CM3 model, particularly in portions of the Upper Bay and parts of the Mid Bay,

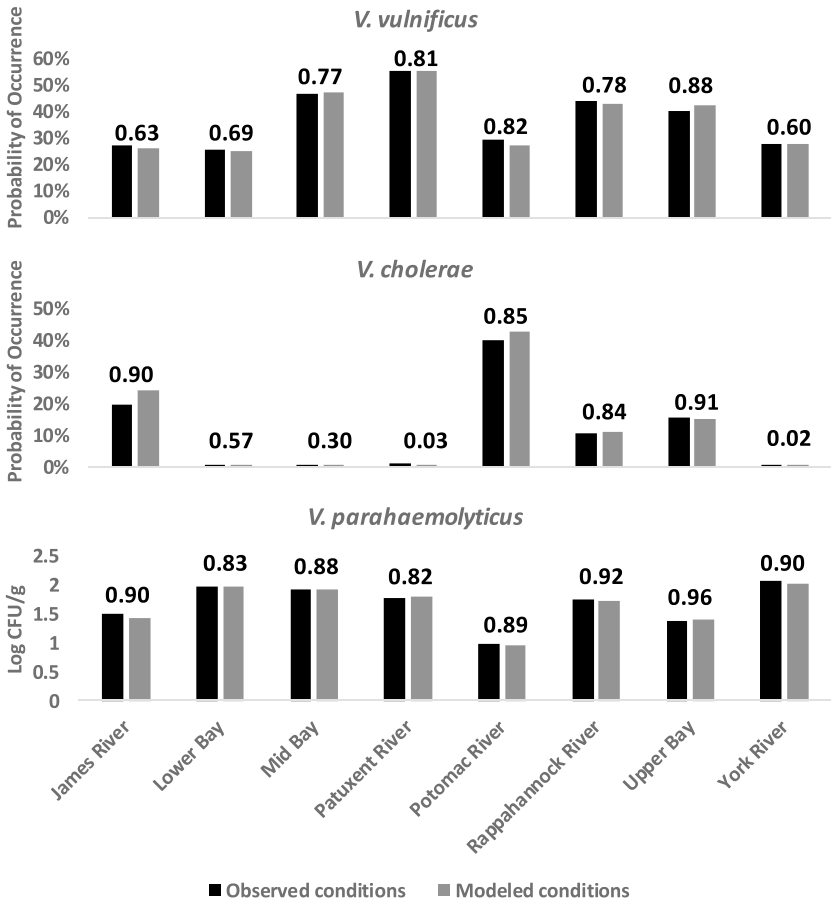

Figure 4. Estimated probability of occurrence (*V. vulnificus* and *V. cholerae*) and concentration of *V. parahaemolyticus* in oysters (log), in each region of the Chesapeake Bay, from GLMs in Table 1. Temperature and salinity values are sourced from CTD casts (black bars) and estimates from the statistical framework in Figure 3 at the same locations (gray bars), during seasons of highest detectability (May–October for *V. vulnificus* and *V. parahaemolyticus*, March–August for *V. cholerae*). R^2 values between GLM predictions for each species from CTD casts and the statistical framework from within each region are shown. Note that only out-of-model test years (2006–2015) were used [see *Muhling et al.*, 2017].

where mean probabilities of occurrence increased by more than 20% over late twentieth century levels. Projected increases were about half this size for the MRI model but similar in spatial character.

In contrast, projections for the probability of occurrence of *V. cholerae* showed a very similar spatial distribution between the historical and future spring-summer time periods (Figure 7).

While probabilities of occurrence increased within high-risk areas, the minimal changes to summer salinity fields projected by the GCMs kept these areas restricted to the northern Upper Bay and upper reaches of the James and Potomac Rivers, where salinities remained low. Projections from the drier IPSL model also suggested an upstream contraction of high-risk areas due to increasing salinities in currently mesohaline to oligohaline regions of the bay. This pattern was not evident in the wetter CM3 model.

The mean modeled concentration of *V. parahaemolyticus* CFU/(log) in oysters during summer was projected to increase between the historical and future time periods, particularly in the warmer CM3 model. In contrast to *V. cholerae*, high-risk areas for *V. parahaemolyticus* spread across most of the Chesapeake Bay, with the exception of low salinity areas in the Upper Bay and upper reaches of rivers (Figure 8). Increases in future high-risk areas were more spatially uniform than for *V. cholerae* but were slightly higher in the upper bay and the midreaches of the major rivers.

The projected increases in probability of occurrence of *V. vulnificus* varied somewhat among different zones of the Chesapeake Bay (Figure 9). The Mid Bay was projected to show the greatest increase: from

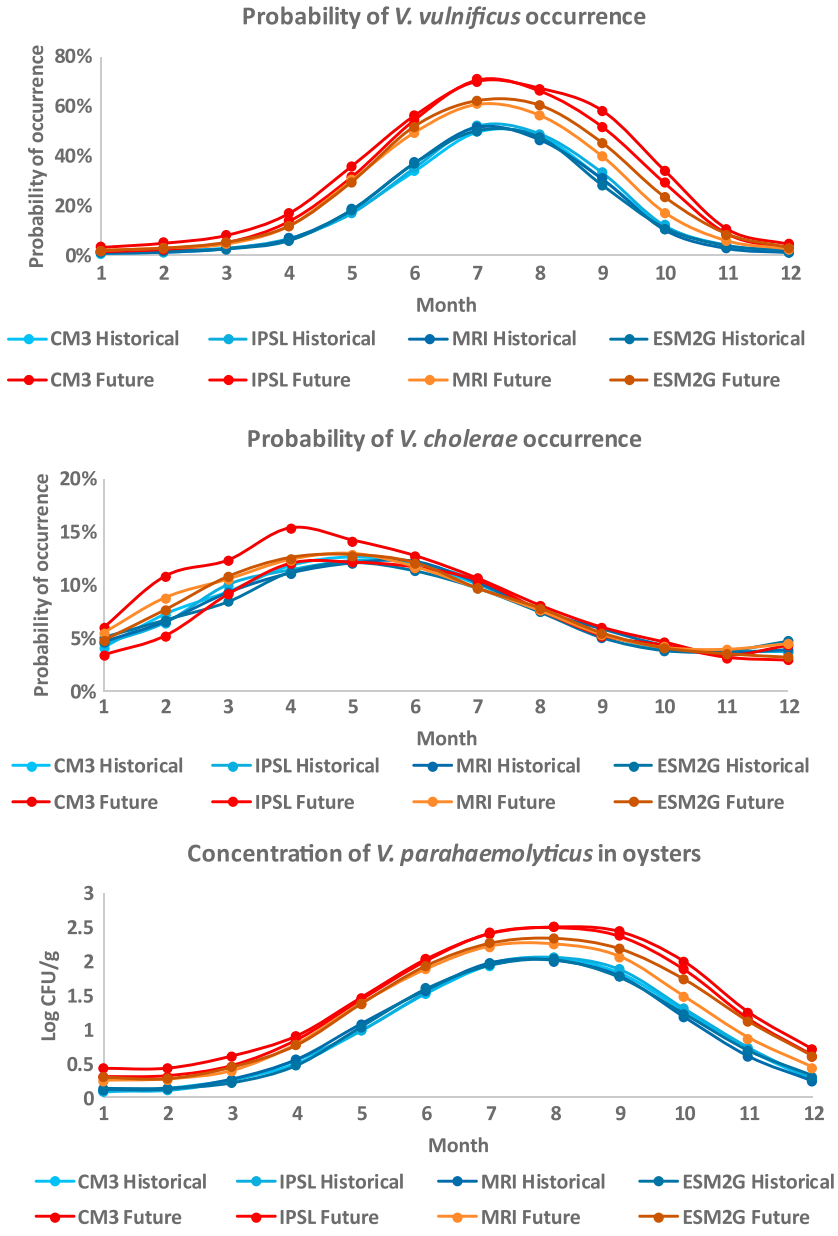

Figure 5. Mean monthly probability of occurrence for (top) *V. vulnificus* and (middle) *V. cholerae*, and predicted mean (bottom) *V. parahaemolyticus* in oysters, between a historical (1970–1999) and future (2071–2100) time period, across all regions of the Chesapeake Bay. Projections were calculated using the GLMs in Table 1, using four statistically downscaled GCMs.

a mean probability of occurrence of 47.3% in 1970–1999 to a mean of 71.7% by 2071–2100 during the peak summer season. Increases in the Lower Bay and Patuxent River were weaker. The Lower Bay remained the lowest risk zone, with probability of occurrence of *V. vulnificus* increasing from 21.2% to 41.0% by the end of the 21st century. Conversely, the Patuxent River remained the highest risk zone: increasing from 64.6% to 84.2%.

Projected increases in *V. parahaemolyticus* were the most spatially uniform of the three species, with little difference among zones (Figure 9). The Lower Bay showed slightly smaller increases due to the moderating influence of the continental shelf environment on water temperatures in this area, but all other zones were similar to each other. As with *V. vulnificus*, the variability in projections contributed by the warmer CM3 model versus the cooler MRI model was clearly evident.

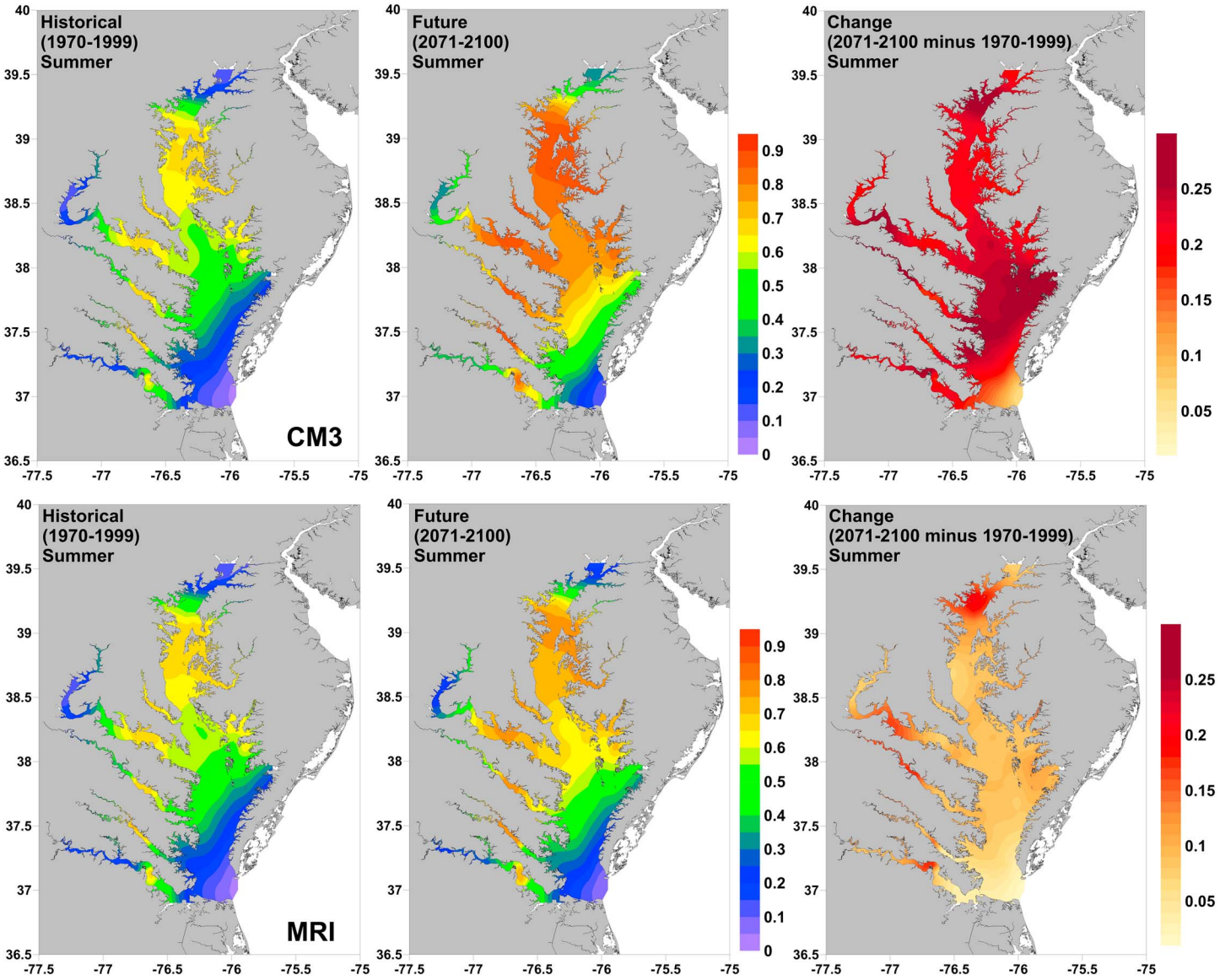

Figure 6. Projections of historical (1970–1999) and future (2071–2100) probability of summer (July–September) *V. vulnificus* occurrence in the Chesapeake Bay from two statistically downscaled GCMs (CM3 and MRI). The change between the two time periods is also shown.

In contrast to the more uniform increases projected for the other two species, projected changes in probability of occurrence of *V. cholerae* were much more spatially complex (Figure 9). Zones with historically low probabilities of occurrence largely remained so during the spring-summer peak season, due to the restriction of this species to low salinity regions. In zones with historically higher concentrations of *V. cholerae*, probabilities of occurrence were projected to increase in the wetter CM3 model but to decrease in the drier IPSL model.

4. Discussion

4.1. Climate Change and *Vibrio* Risk

Several previous studies have hypothesized direct and indirect effects of climate on *Vibrio* presence and disease risk. The most studied species is undoubtedly *V. cholerae*. Strains O1 and O139 can cause epidemic disease outbreaks, and studies from different regions around the world have correlated these to air and water temperature, rainfall, river discharge, and phytoplankton/zooplankton abundance and composition [*Colwell*, 1996; *Lobitz et al.*, 2000; *Rodó et al.*, 2002; *Gil et al.*, 2004; *Koelle et al.*, 2005; *Greer et al.*, 2008;

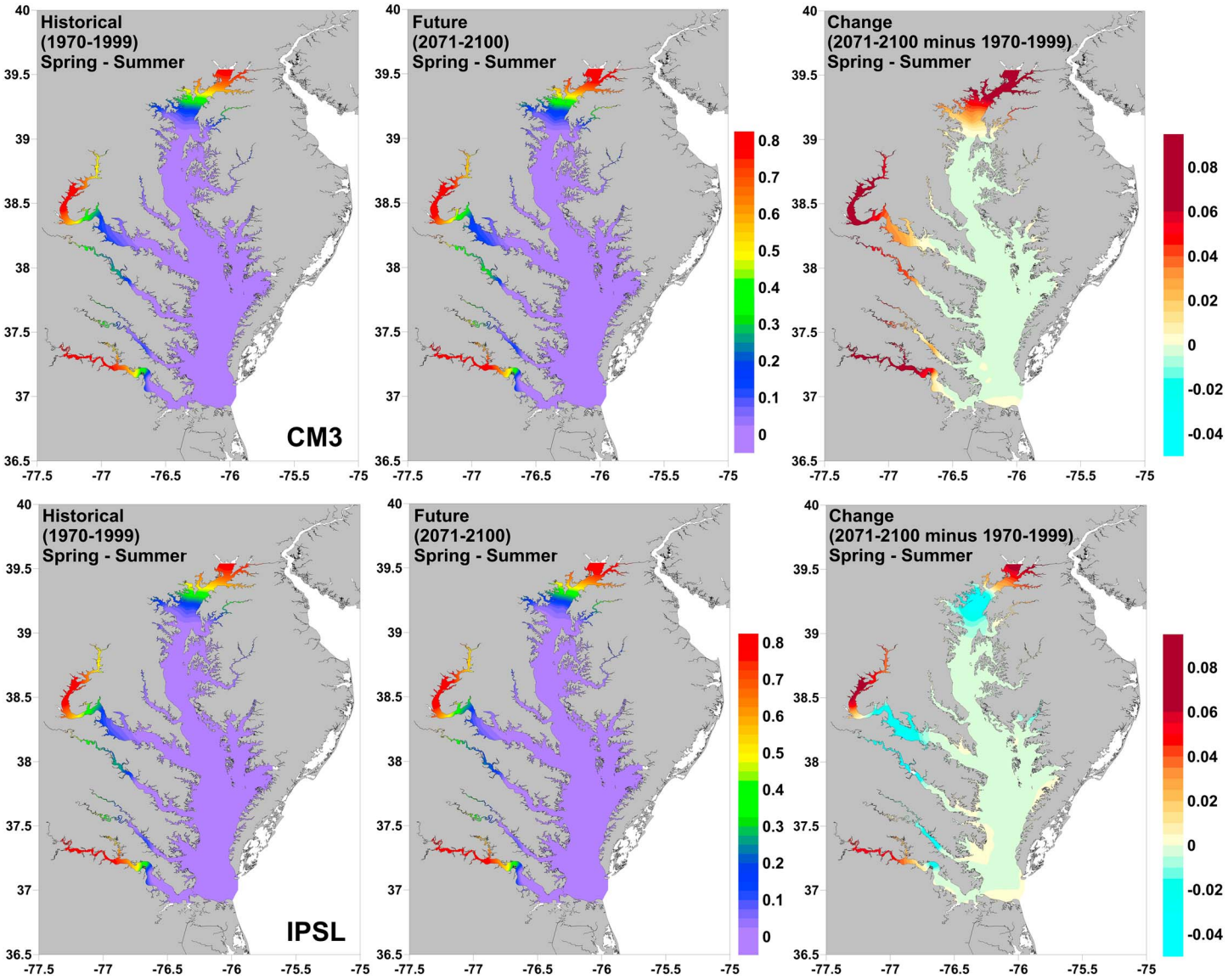

Figure 7. Projections of historical (1970–1999) and future (2071–2100) probability of spring-summer (March–September) *V. cholerae* occurrence in the Chesapeake Bay from two statistically downscaled GCMs (CM3 and IPSL). The change between the two time periods is also shown.

Constantin de Magny et al., 2012]. Some analyses have suggested that climate change-induced warming and eutrophication may exacerbate cholera outbreaks, with changing river flow patterns and flood events also potentially important [*Martinez-Urtaza et al.*, 2010; *Tirado et al.*, 2010].

Recent work has highlighted increasing trends of *Vibrio* species occurrence and related infections in many areas around the world [e.g., *Pascual et al.*, 2000; *Martinez-Urtaza et al.*, 2010; *Tirado et al.*, 2010; *Vezzulli et al.*, 2010a, 2016; *Newton et al.*, 2012; *Baker-Austin et al.*, 2013]. There have also been cases of largely unprecedented occurrence of *Vibrio* infections in some parts of Europe, the Atlantic coast of the United States, and Alaska in recent years, associated with positive temperature anomalies and heat waves [*McLaughlin et al.*, 2005; *Paz et al.*, 2007; *Lima and Wethey*, 2012; *Baker-Austin et al.*, 2013; *Vezzulli et al.*, 2016]. Several studies have shown convincing links between recent warming temperatures and associated outbreaks of *Vibrio* illness, including in some areas where it was previously rare or unknown [*Baker-Austin et al.*, 2017]. This suggests great potential for future climate change to increase habitat availability, season length, and infection rates from *Vibrios*. There may also be increases in associated economic costs from health care and lost wages, and increases in regulatory costs for some sectors of the seafood industry.

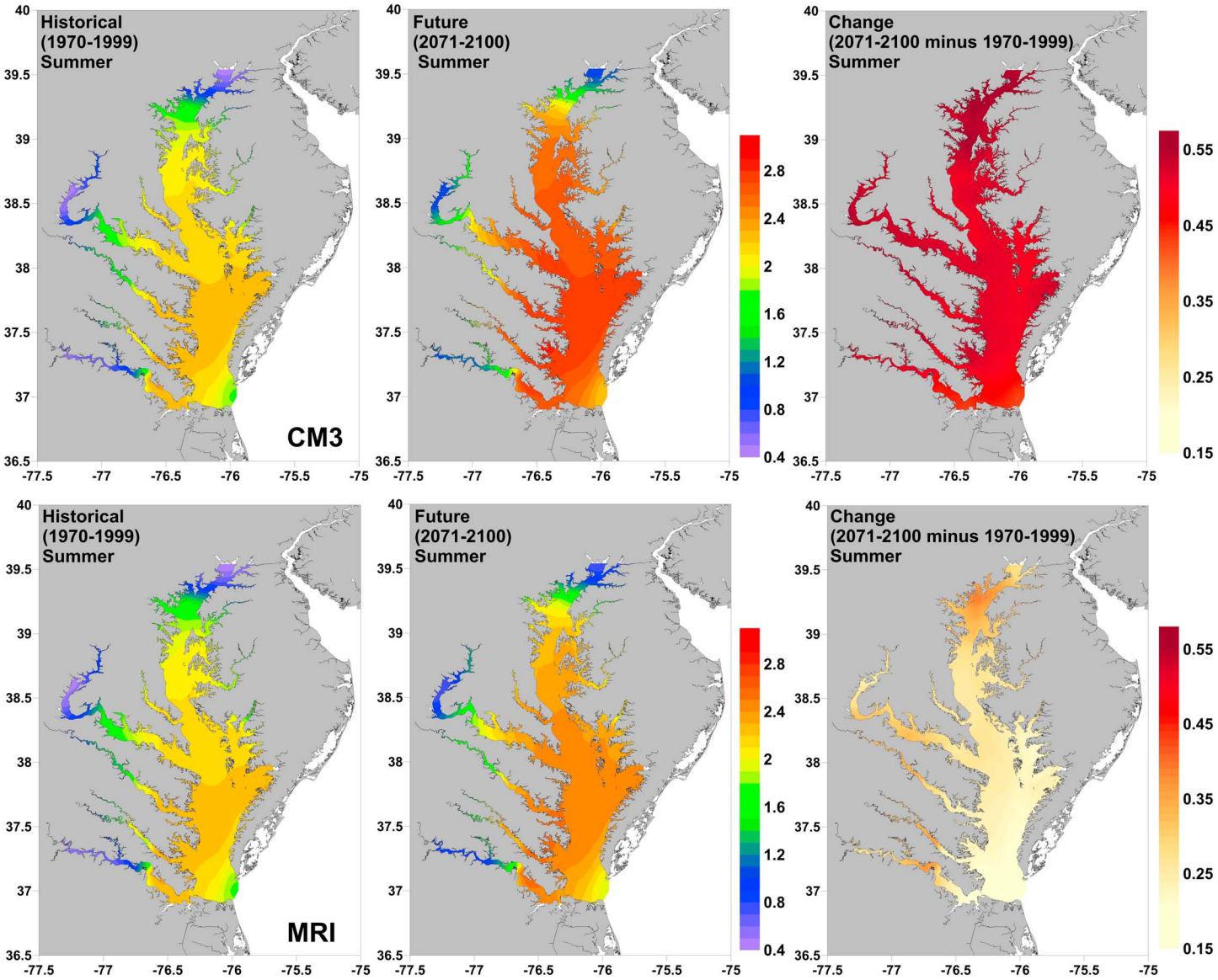

Figure 8. Projections of historical (1970–1999) and future (2071–2100) mean concentration of summer (July–September) *V. parahaemolyticus* in oysters in the Chesapeake Bay from two statistically downscaled GCMs (CM3 and MRI). The change between the two time periods is also shown.

However, there are few studies looking at risk of future *Vibrio* species occurrence or infection using projections from IPCC climate models. This may be partially due to the spatial resolution required. Some brackish waters with high *Vibrio* risk are poorly resolved at the native resolution of most GCMs (~1–2°). The difficulties inherent in projecting future salinity fields in estuarine and nearshore environments may also have been limited. For example, *Jacobs et al.* [2015] projected a temperature-driven increase in season length for *V. vulnificus* in the Chesapeake Bay over the next century, consistent with the present study. However, these authors used a fixed value for salinity, because no estuary-scale projections were available. We addressed the two challenges raised above (spatial resolution and lack of salinity projections) by using a spatial modeling framework, which ingests statistically downscaled projections of air temperature and precipitation [*Muhling et al.*, 2017]. Present-day predictions of *Vibrio* probability of occurrence or concentration using modeled temperature and salinity from the statistical framework were close to those using in situ CTD casts. As a result, we can have some confidence that the framework approach is reasonable for use in developing future spatial projections of *Vibrios* in the Chesapeake Bay.

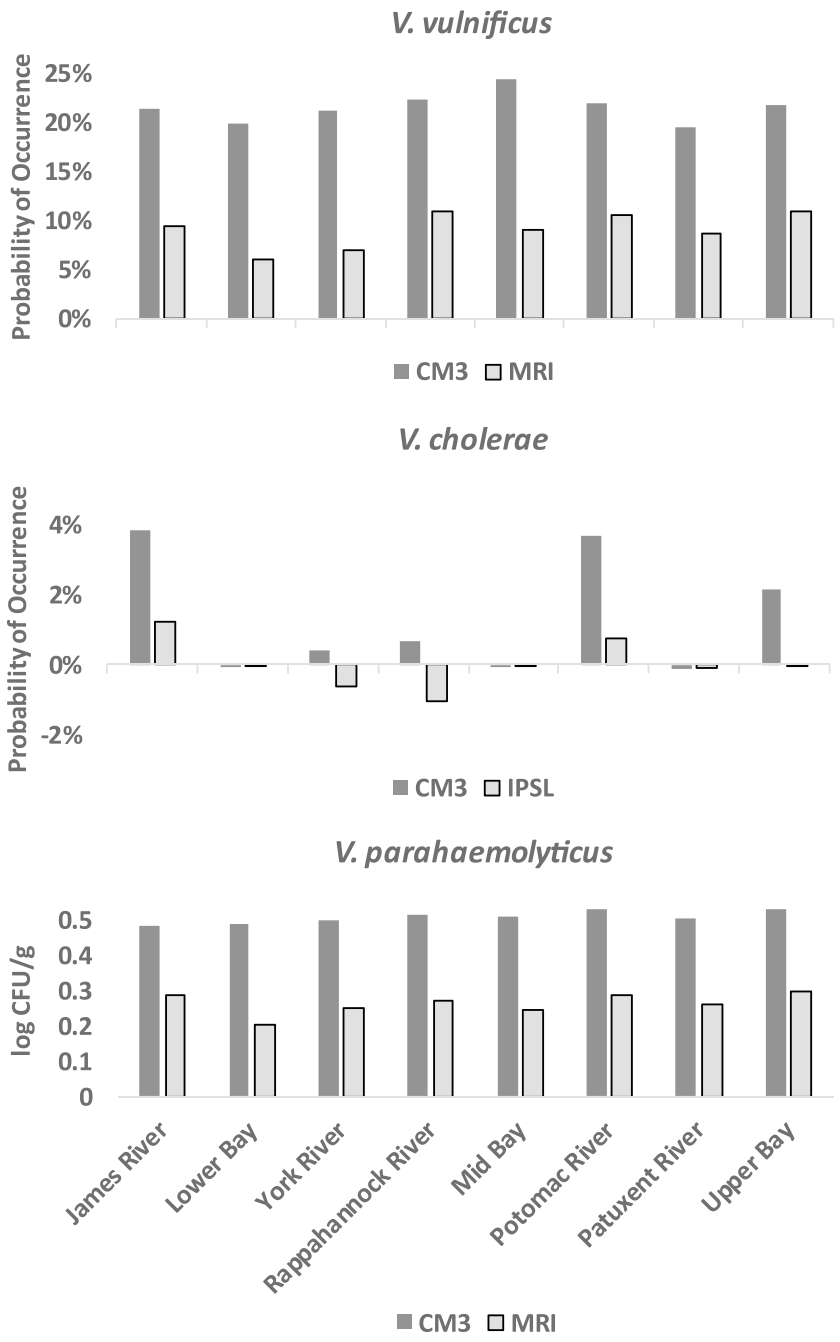

Figure 9. Change in mean probability of occurrence (*V. vulnificus* and *V. cholerae*) and concentration of *V. parahaemolyticus* in oysters (log), between historical (1970–1999) and future (2071–2100) time periods in each zone of the Chesapeake Bay. Only projections for peak seasons (summer for *V. vulnificus* and *V. parahaemolyticus*, spring-summer for *V. cholerae*) are shown.

4.2. Future Projections

Results from future projections of *Vibrio* habitat in the Chesapeake Bay highlighted considerable interspecific variability. Probability of *V. vulnificus* occurrence increased markedly across the Bay during the peak summer season, and the overall area of high probability expanded. Increases were stronger in the warmer CM3 model than in the less warm MRI model, but the direction of change was consistent.

Similarly, the mean predicted concentration of *V. parahaemolyticus* in oysters increased throughout much of the Bay. Accounting for the log scale of predictions, projections from the MRI model showed

V. parahaemolyticus concentrations increasing by 1.5 times, while the CM3 model suggested that concentrations would more than triple. This species had the broadest modeled environmental tolerances of all three *Vibrios* examined, with positive concentrations predicted at salinities from 0 to 31 psu and temperatures of greater than ~10°C, although concentrations were highest at warm temperatures (> 25°C) and moderate salinities (5–25 psu). The environmental range of *V. parahaemolyticus* is thus approximately the same as for the oysters it is associated with [*Galtsoff*, 1964; *Mann and Powell*, 2007].

In contrast to the other two species, the observed salinity association of *V. cholerae* restricted their distribution to the upper portions of the Chesapeake Bay and major rivers, with little expansion of habitat under climate change. Mean bay-wide projected probabilities of occurrence during late winter and spring increased in the wetter CM3 model, increased slightly in the MRI and ESM2G models, and decreased slightly in the drier IPSL model. Projections for this species also showed the greatest spatial complexity. While projected probabilities of occurrence increased most strongly in the James and Potomac Rivers, they remained low in most other areas and even decreased somewhat in the Rappahannock and York Rivers in the drier IPSL model.

Projections of *V. vulnificus* differed somewhat among the different zones of the Chesapeake Bay, although to a lesser extent than *V. cholerae*. The strongest increase was in the Mid Bay, suggesting a down-bay extension of current high-risk areas. Projected increases in *V. parahaemolyticus* were the most spatially uniform of the three species. While the nature of the temperature relationships in the GLMs thus determined the general scale of future increase for all three *Vibrio* species, the relationships with salinity determined the spatial patterns of this increase. This result highlights the importance of salinity fields for sensitive species, if projections of future high-risk hot spots are a priority.

4.3. Using Different Biological Habitat Models

While the use of correlative habitat models in climate change impact studies is common, the effect of model choice and parameterization on results is not often considered. However, recent work suggests that the choice of biological model can be influential [*Jones et al*., 2012; *Payne et al*., 2015]. Even where habitat models give very similar results on present-day data, they can diverge substantially once extrapolated beyond the range of the training data. This is commonly required when projecting temperature-based habitat models under future climate change scenarios.

The present study relied on previously existing GLMs to predict *Vibrio* occurrence or abundance. However, *Urquhart et al*. [2014] noted that a GLM for *V. vulnificus* trained on a subset of the data from *Jacobs et al*. [2010] (an earlier version of the GLM described in *Jacobs et al*. [2014]) gave substantially different results to a GLM trained on samples collected in the upper Chesapeake Bay over a different time period (2011–2012). In addition, a Generalized Additive Model (GAM) trained on the latter data set gave different results to both GLMs, primarily due to the fact that GAMs allow nonlinear response curves [*Züur et al*., 2009]. *Urquhart et al*. [2014] thus concluded that the impacts of climate change on *V. vulnificus* in the Chesapeake Bay could not be projected with any useful certainty.

As the findings of *Urquhart et al*. [2014] are strongly relevant to the current study, we reevaluated the robustness of our results using the full 2007–2010 data set for *V. vulnificus* from *Jacobs et al*. [2014]. The GLM in Table 1 was compared to two GAMs with logit link functions built using the mgcv package in R 3.2.1 [*Wood*, 2006; *R Core Team*, 2015]. As the number of "knots" for polynomial smoothers affects the shapes of response curves in GAMs [*Keele*, 2008; *Züur et al*., 2009] we built two models, with the maximum number of knots for both temperature and salinity set at three (GAM3) and then at five (GAM5). These values were within the range of sensible values recommended by *Keele* [2008], and both generated biologically plausible but slightly different response curves for both temperature and salinity.

In contrast to *Urquhart et al*. [2014], the three *V. vulnificus* habitat models (GLM, GAM3, and GAM5) gave similar seasonal predictions for the late twentieth century (Figure 10). This was likely due to the broader spatiotemporal extent of the field data available to us, compared to *Urquhart et al*. [2014] which emphasizes the advantages of using comprehensive data sets for habitat model training. The slightly different shapes of the modeled temperature response curves did result in diverging projections of future probability of occurrence by the late 21st century. Importantly, however, all showed a temperature-driven increase. Laboratory experiments suggest optimum temperatures for *Vibrio* species of 37–39°C [*Kelly*, 1982; *Miles et al*., 1997; *Sedas*, 2007]: much warmer than currently observed conditions in the Chesapeake Bay. In addition, recent

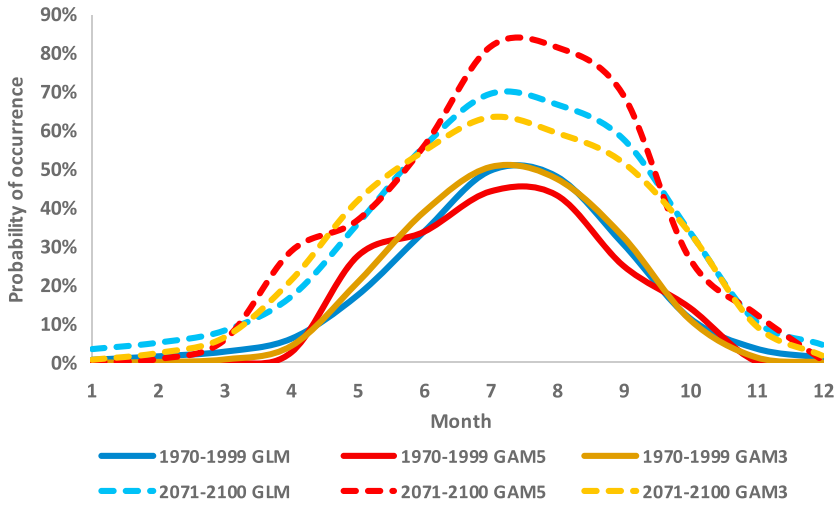

Figure 10. Monthly modeled probability of occurrence for *V. vulnificus* between a historical (1970–1999) and a future (2071–2100) time period. Projections are compared between a published GLM [*Jacobs et al.*, 2014] (Table 1) and two GAMs and were calculated using statistically downscaled outputs from the CM3 GCM.

warming conditions have resulted in increasing rates of *Vibrio*-associated illness in other parts of the world [*Andersson and Ekdahl*, 2006; *Paz et al.*, 2007; *Martinez-Urtaza et al.*, 2010; *Vezzulli et al.*, 2010a, 2016; *Baker-Austin et al.*, 2013; *Le Roux et al.*, 2015]. If other environmental conditions remain favorable, it therefore seems reasonable to assume that warming conditions will favor *Vibrios* and that generally positive temperature response curves are appropriate.

4.4. Management Implications

A primary management issue associated with *Vibrio*-related illnesses is the economic costs of health care to affected patients. Both *V. vulnificus* and *V. parahaemolyticus* infections currently lead to millions of dollars in associated treatment costs in the United States: the former because of its severity and the latter because of its high frequency [*Ralston et al.*, 2011; *Scallan et al.*, 2011; *Hoffmann et al.*, 2015]. Results from this study suggest substantially increased risk of *V. vulnificus* in Chesapeake Bay waters under climate change and increasing mean concentration of *V. parahaemolyticus* in oysters. Although the economic burden of these trends is difficult to estimate without information on virulence, future population density and recreational use of the region, and future oyster harvest rates, the potential for increasing rates of illness is a serious prospect.

In addition, best practices for the oyster harvesting industry may no longer be effective as water temperatures continue to warm. At present, Maryland and Virginia *Vibrio* control plans require that fishers deliver harvested oysters to dealers by certain times of day and refrigerate their catch within a certain number of hours, depending on the month [e.g., *Virginia Department of Health*, 2016]. These are earlier/shorter in warmer months, and later/longer in cooler months, respectively. If climate change-induced warming leads to higher concentrations of *V. parahaemolyticus* in oysters, then current restrictions will likely have to be adjusted, to avoid unacceptably contaminated product and increased rates of illness.

4.5. Uncertainties and Future Work

In addition to the sources of uncertainty mentioned above, a major missing piece of the current projections is the lack of biological variables. Phytoplankton and zooplankton have been shown to be important to *Vibrio* ecology (especially *V. cholerae*), and chitinous zooplankton in particular may act as a reservoir for some species [*Kaneko and Colwell*, 1973, 1975; *Huq et al.*, 1983; *Rawlings et al.*, 2007; *Gil et al.*, 2004; *Vezzulli et al.*, 2010b; *Turner et al.*, 2014; *Constantin de Magny et al.*, 2011; *Main et al.*, 2015].

Another consideration, which is common to many climate change impact studies, is that the environmental relationships shown by the habitat models may not represent the full extent of physiological limits. This is particularly evident for *V. cholerae*. While the habitat model developed by *Louis et al.* [2003] shows a

strong association between *V. cholerae* and low salinity waters, this species is known to tolerate much broader salinities in other regions and in the laboratory [*Singleton et al*., 1982a, 1982b; *Constantin De Magny et al*., 2009; *Banakar et al*., 2011]. *Louis et al*. [2003] noted that other field and laboratory studies had found varying optimum salinity values for *V. cholerae*, and that their modeled salinity relationships for the Chesapeake Bay may have been proxies for other biologically important factors, such as turbidity or nutrient loads. While phytoplankton and zooplankton substrates are known to be important for *V. cholerae*, *Louis et al*. [2003] found no strong relationships between the occurrence of *V. cholerae* in the Chesapeake Bay and concentrations of chlorophyll α, or of specific zooplankton groups (e.g., copepods, rotifers, and barnacle nauplii). As a result, although the strongest predictors for *V. cholerae* in the Chesapeake Bay are currently temperature and salinity, the precise mechanisms controlling *V. cholerae* in the Chesapeake Bay remain somewhat unclear.

It is also important to note that environmental concentrations of *Vibrio* species do not necessarily predict disease risk, although the two are often correlated [*Baker-Austin et al*., 2013; *Vezzulli et al*., 2016]. Some studies have recorded an increase in *Vibrio* infections in the past few decades [*Scallan et al*., 2011; *Newton et al*., 2012]. However, it is not yet clear if these are due to changing environmental conditions. Biogeochemical factors (e.g., nutrient concentrations, phytoplankton or zooplankton abundance, or community structure) and the presence of particular strains or virulence-correlated genes may be more important for interannual disease risk than simple probability of occurrence. *Jacobs et al*. [2014] found that occurrence of a virulence-correlated gene (*Vcg*) in *V. vulnificus* in the Chesapeake Bay was associated not only with temperature and salinity but also with nutrient and chlorophyll concentrations, which were not modeled in our study.

Projections of *V. parahaemolyticus* in oysters assume that suitable habitats of the Chesapeake Bay will continue to support oyster production. Although *C. virginica* has relatively broad environmental tolerances, populations have been strongly and negatively affected by habitat loss, eutrophication, and disease in recent decades [*Rothschild et al*., 1994]. It is therefore difficult to project the extent of oyster habitat, and the associated state of the oyster fishery, at the middle to end of the century with any confidence.

The use of the statistical framework to derive temperature and salinity in the Chesapeake Bay introduces additional uncertainty to the projections. These are discussed in more depth in *Muhling et al*. [2017], but relate primarily to the assumption of stationarity in statistically downscaled projections [e.g., *Vrac et al*., 2007; *Gaitan and Cannon*, 2013; *Gaitan et al*., 2014; *Gaitan*, 2016; *Dixon et al*., 2016], the simplicity of the water balance model and error from the model trees used to create the spatial fields.

Another source of uncertainty which requires further study is the interaction between future demographics and disease risk. As the United States population continues to increase and age [*Ortman and Guarneri*, 2009], more people may be exposed to *Vibrio* pathogens. An aging population, particularly with increasing prevalence of existing health conditions, may increase susceptibility, health care costs, and risk of death [*Ralston et al*., 2011; *Weis et al*., 2011].

While our projections were specific to the Chesapeake Bay, this approach may be useful in other regions of the world. Other parts of the northeast United States and northwest Europe, in particular, have been warming rapidly over the past several decades [*Lima and Wethey*, 2012]. Similar methods to those used in this study could be applied to assess future *Vibrio* prevalence in higher-risk areas or to assess the probability of emergence of new areas of disease risk.

5. Conclusions

Overall, we found that future climate change is likely to increase the probability of occurrence of *V. vulnificus* in the Chesapeake Bay and increase the mean concentration of *V. parahaemolyticus* in oysters by the end of the 21st century. In contrast, probabilities of occurrence for *V. cholerae* were projected to increase only in the wetter GCMs, and high-risk areas remained restricted to low salinity zones of the bay. The length of the high-risk summer season for *V. vulnificus* and *V. parahaemolyticus* was also projected to increase. These findings have implications for recreational use and seafood extraction from the Chesapeake Bay, with the potential for considerable economic costs as a result.

Acknowledgments
The manuscript was significantly improved by comments from J. Dunne and A. Leight. Assistance with the FDA model for *V. parahaemolyticus* was provided by J. Bowers. Primary funding and support for this study were provided by the NOAA National Ocean Service (NOS) National Centers for Coastal Ocean Science (NCCOS), with additional support from the NOAA National Marine Fisheries Service (NMFS) Office of Science and Technology, the NOAA Integrated Ecosystem Assessment (IEA) Program, and the NOAA Office of Oceanic and Atmospheric Research (OAR). Data supporting the conclusions in this study can be found in Table 1 and in the associated published manuscripts cited in the text. Climate change projections can be obtained by contacting the first author.

References

Altekruse, S. F., R. D. Bishop, L. M. Baldy, S. G. Thompson, S. A. Wilson, B. J. Ray, and P. M. Griffin (2000), *Vibrio* gastroenteritis in the US Gulf of Mexico region: The role of raw oysters, *Epidemiol. Infect.*, *124*, 489–495.

Andersson, Y., and K. Ekdahl (2006), Wound infections due to *Vibrio cholerae* in Sweden after swimming in the Baltic Sea, summer 2006, *Eurosurveillance*, *11*, E060803.

Baker-Austin, C., L. Stockley, R. Rangdale, and J. Martinez-Urtaza (2010), Environmental occurrence and clinical impact of *Vibrio vulnificus* and *Vibrio parahaemolyticus*: A European perspective, *Environ. Microbiol. Rep.*, *2*, 7–18.

Baker-Austin, C., J. A. Trinanes, N. G. Taylor, R. Hartnell, A. Siitonen, and J. Martinez-Urtaza (2013), Emerging *Vibrio* risk at high latitudes in response to ocean warming, *Nat. Clim. Change*, *3*, 73–77.

Baker-Austin, C., J. Trinanes, N. Gonzalez-Escalona, and J. Martinez-Urtaza (2017), Non-cholera *Vibrios*: The microbial barometer of climate change, *Trends Microbiol.*, *25*, 76–84.

Banakar, V., G. Constantin De Magny, J. Jacobs, R. Murtugudde, A. Huq, R. J. Wood, and R. R. Colwell (2011), Temporal and spatial variability in the distribution of *Vibrio vulnificus* in the Chesapeake Bay: A hindcast study, *EcoHealth*, *8*, 456–467.

Chávez, M. D. R. C., V. P. Sedas, E. O. Borunda, and F. L. Reynoso (2005), Influence of water temperature and salinity on seasonal occurrences of *Vibrio cholerae* and enteric bacteria in oyster-producing areas of Veracruz, México, *Mar. Pollut. Bull.*, *50*, 1641–1648.

Chen, M., W. Shi, P. Xie, V. Silva, V. E. Kousky, R. W. Higgins, and J. E. Janowiak (2008), Assessing objective techniques for gauge-based analyses of global daily precipitation, *J. Geophys. Res.*, *113*, D04110, doi:10.1029/2007JD009132.

Colwell, R. R. (1996), Global climate and infectious disease: The cholera paradigm, *Science*, *274*, 2025–2031.

Colwell, R. R., J. Kaper, and S. W. Joseph (1977), *Vibrio cholerae*, *Vibrio parahaemolyticus*, and other *Vibrios*: Occurrence and distribution in Chesapeake Bay, *Science*, *198*, 394–396.

Constantin de Magny, G., W. Long, C. W. Brown, R. R. Hood, A. Huq, R. Murtugudde, and R. R. Colwell (2009), Predicting the distribution of *Vibrio* spp. in the Chesapeake Bay: A *Vibrio cholerae* case study, *EcoHealth*, *6*, 378–389.

Constantin de Magny, G., P. K. Mozumder, C. J. Grim, N. A. Hasan, M. N. Naser, M. Alam, R. B. Sack, A. Huq, and R. R. Colwell (2011), Role of zooplankton diversity in *Vibrio cholerae* population dynamics and in the incidence of cholera in the Bangladesh Sundarbans, *Appl. Environ. Microbiol.*, *77*, 6125–6132.

Constantin de Magny, G., W. Thiaw, V. Kumar, N. M. Manga, B. M. Diop, L. Gueye, M. Kamara, B. Roche, R. Murtugudde, and R. R. Colwell (2012), Cholera outbreak in Senegal in 2005: Was climate a factor?, *PLoS One*, *7*, e44577, doi:10.1371/journal.pone.0044577.

Dixon, K. W., J. R. Lanzante, M. J. Nath, K. Hayhoe, A. Stoner, A. Radhakrishnan, V. Balaji, and C. F. Gaitán (2016), Evaluating the stationarity assumption in statistically downscaled climate projections: Is past performance an indicator of future results?, *Clim. Change*, *135*, 395–408.

Donner, L. J., et al. (2011), The dynamical core, physical parameterizations, and basic simulation characteristics of the atmospheric component AM3 of the GFDL global coupled model CM3, *J. Clim.*, *24*, 3484–3519.

Dufresne, J.-L., et al. (2013), Climate change projections using the IPSL-CM5 Earth System Model: From CMIP3 to CMIP5, *Clim. Dyn.*, *40*, 2123–2165.

Dunne, J. P., et al. (2012), GFDL's ESM2 global coupled climate-carbon Earth system models. Part I: Physical formulation and baseline simulation characteristics, *J. Clim.*, *2*, 6646–6665.

Fan, Y., and H. van den Dool (2008), A global monthly land surface air temperature analysis for 1948-present, *J. Geophys. Res.*, *113*, D01103, doi:10.1029/2007JD008470.

Farmer, J. J., III, J. M. Janda, F. W. Brenner, D. N. Cameron, and K. M. Birkhead (2005), Genus I. *Vibrio* Pacini 1854, 411AL, *Bergey's Manual Syst. Bacteriol.*, *2B*, 494–546.

Gaitan, C. F. (2016), Effects of variance adjustment techniques and time-invariant transfer functions on heat wave duration indices and other metrics derived from downscaled time-series. Study case: Montreal, Canada, *Nat. Hazards*, *83*, 1661–1681.

Gaitan, C. F., and A. J. Cannon (2013), Validation of historical and future statistically downscaled pseudo-observed surface wind speeds in terms of annual climate indices and daily variability, *Renew. Energy*, *51*, 489–496.

Gaitan, C. F., W. W. Hsieh, and A. J. Cannon (2014), Comparison of statistically downscaled precipitation in terms of future climate indices and daily variability for southern Ontario and Quebec, Canada, *Clim. Dyn.*, *43*, 3201–3217.

Galtsoff, P. S. (1964), The American oyster *Crassostrea virginica* Gmelin, *Fish. Bull.*, *64*, 1–480.

Gil, A. I., et al. (2004), Occurrence and distribution of *Vibrio cholerae* in the coastal environment of Peru, *Environ. Microbiol.*, *6*, 699–706.

Greer, A., V. Ng, and D. Fisman (2008), Climate change and infectious diseases in North America: The road ahead, *Can. Med. Assoc. J.*, *178*, 715–722.

Haley, B. J., et al. (2014), Molecular diversity and predictability of *Vibrio parahaemolyticus* along the Georgian coastal zone of the Black Sea, *Front. Microbiol.*, *5*, 171–179.

Hoffmann, S., B. Maculloch, and M. Batz (2015), Economic burden of major foodborne illnesses acquired in the United States, *United States Department of Agriculture Economic Research Service Economic Information Bulletin*, 140, May 2015, 59p.

Huq, A., E. B. Small, P. A. West, M. I. Huq, R. Rahman, and R. R. Colwell (1983), Ecological relationships between *Vibrio cholerae* and planktonic crustacean copepods, *Appl. Environ. Microbiol.*, *45*, 275–283.

Huq, A., P. A. West, E. B. Small, M. I. Huq, and R. R. Colwell (1984), Influence of water temperature, salinity, and pH on survival and growth of toxigenic *Vibrio cholerae* serovar 01 associated with live copepods in laboratory microcosms, *Appl. Environ. Microbiol.*, *48*, 420–424.

Jacobs, J. M., M. Rhodes, C. W. Brown, R. R. Hood, A. Leight, W. Long, and R. Wood (2010), Predicting the distribution of *Vibrio vulnificus* in Chesapeake Bay, *NOAA Technical Memorandum NOA NCCOS* 112, 24p.

Jacobs, J. M., M. Rhodes, C. W. Brown, R. R. Hood, A. Leight, W. Long, and R. Wood (2014), Modeling and forecasting the distribution of *Vibrio vulnificus* in Chesapeake Bay, *J. Appl. Microbiol.*, *117*, 1312–1327.

Jacobs, J., S. K. Moore, K. E. Kunkel, and L. Sun (2015), A framework for examining climate-driven changes to the seasonality and geographical range of coastal pathogens and harmful algae, *Clim. Risk Manag.*, *8*, 16–27.

Jiang, S. C., and W. Fu (2001), Seasonal abundance and distribution of *Vibrio cholerae* in coastal waters quantified by a 16S-23S intergenic spacer probe, *Microb. Ecol.*, *42*, 540–548.

Jones, E. H., K. A. Feldman, A. Palmer, E. Butler, D. Blythe, and C. S. Mitchell (2013), *Vibrio* infections and surveillance in Maryland, 2002–2008, *Public Health Rep.*, *128*, 537–545.

Jones, M. C., S. R. Dye, J. K. Pinnegar, R. Warren, and W. W. Cheung (2012), Modelling commercial fish distributions: Prediction and assessment using different approaches, *Ecol. Model.*, *225*, 133–145.

Kaneko, T., and R. R. Colwell (1973), Ecology of *Vibrio parahaemolyticus* in Chesapeake Bay, *J. Bacteriol.*, *113*, 24–32.

Kaneko, T., and R. R. Colwell (1975), Adsorption of *Vibrio parahaemolyticus* onto chitin and copepods, *J. Appl. Microbiol.*, *29*, 269–274.

Kaspar, C. W., and M. L. Tamplin (1993), Effects of temperature and salinity on the survival of *Vibrio vulnificus* in seawater and shellfish, *Appl. Environ. Microbiol.*, *59*, 2425–2429.
Keele, L. J. (2008), *Semiparametric Regression for the Social Sciences*, John Wiley, Chichester, U. K.
Kelly, M. T. (1982), Effect of temperature and salinity on *Vibrio* (Beneckea) *vulnificus* occurrence in a Gulf Coast environment, *Appl. Environ. Microbiol.*, *44*, 820–824.
Koelle, K., X. Rodó, M. Pascual, M. Yunus, and G. Mostafa (2005), Refractory periods and climate forcing in cholera dynamics, *Nature*, *436*, 696–700.
Kuhn, M. S., S. Weston, C. Keefer, and Coulter N (2015), Cubist: Rule- and instance-based regression modeling, R package version 0.0.18. [Available at http://CRAN.R-project.org/package=Cubist.]
Le Roux, F. L., et al. (2015), The emergence of *Vibrio* pathogens in Europe: Ecology, evolution, and pathogenesis (Paris, 11–12th March 2015), *Front. Microbiol.*, *6*, 830, doi:10.3389/fmicb.2015.00830.
Letcher, B. H., D. J. Hocking, K. O'Neil, A. R. Whiteley, K. H. Nislow, and M. J. O'Donnell (2016), A hierarchical model of daily stream temperature using air-water temperature synchronization, autocorrelation, and time lags, *Peer J*, *4*, e1727, doi:10.7717/peerj.1727.
Lima, F. P., and D. S. Wethey (2012), Three decades of high-resolution coastal sea surface temperatures reveal more than warming, *Nat. Commun.*, *3*, 704.
Lipp, E. K., C. Rodriguez-Palacios, and J. B. Rose (2001), Occurrence and distribution of the human pathogen *Vibrio vulnificus* in a subtropical Gulf of Mexico estuary, in *The Ecology and Etiology of Newly Emerging Marine Diseases*, edited by J. W. Porter, pp. 165–173, Springer, Dordrecht, Netherlands.
Lipp, E. K., A. Huq, and R. R. Colwell (2002), Effects of global climate on infectious disease: The cholera model, *Clin. Microbiol. Rev.*, *15*, 757–770.
Lobitz, B., L. Beck, A. Huq, B. Wood, G. Fuchs, A. S. G. Faruque, and R. Colwell (2000), Climate and infectious disease: Use of remote sensing for detection of *Vibrio cholerae* by indirect measurement, *Proc. Natl. Acad. Sci. U.S.A.*, *97*, 1438–1443.
Louis, V. R., E. Russek-Cohen, N. Choopun, I. N. Rivera, B. Gangle, S. C. Jiang, A. Rubin, J. A. Patz, A. Huq, and R. R. Colwell (2003), Predictability of *Vibrio cholerae* in Chesapeake Bay, *Appl. Environ. Microbiol.*, *69*, 2773–2785.
Main, C. R., L. R. Salvitti, E. B. Whereat, and K. J. Coyne (2015), Community-level and species-specific associations between phytoplankton and particle-associated *Vibrio* species in Delaware's inland bays, *Appl. Environ. Microbiol.*, *81*, 5703–5713.
Mann, R., and E. N. Powell (2007), Why oyster restoration goals in the Chesapeake Bay are not and probably cannot be achieved, *J. Shellfish Res.*, *26*, 905–917.
Martinez-Urtaza, J., J. C. Bowers, J. Trinanes, and A. DePaola (2010), Climate anomalies and the increasing risk of *Vibrio parahaemolyticus* and *Vibrio vulnificus* illness, *Food Res. Int.*, *43*, 1780–1790.
Martinez-Urtaza, J., C. Baker-Austin, J. L. Jones, A. E. Newton, G. D. Gonzalez-Aviles, and A. DePaola (2013), Spread of Pacific Northwest *Vibrio parahaemolyticus* strain, *N. Engl. J. Med.*, *369*, 1573–1574.
McCabe, G. J., and S. I. Markstrom (2007), A monthly water-balance model driven by a graphical user interface, *U.S. Geol. Surv. Open File Rep., 2007-1088*, p. 6.
McLaughlin, J. B., A. DePaola, C. A. Bopp, K. A. Martinek, N. P. Napolilli, C. G. Allison, S. L. Murray, E. C. Thompson, M. M. Bird, and J. P. Middaugh (2005), Outbreak of *Vibrio parahaemolyticus* gastroenteritis associated with Alaskan oysters, *N. Engl. J. Med.*, *353*, 1463–1470.
Miles, D. W., T. Ross, J. Olley, and T. A. McMeekin (1997), Development and evaluation of a predictive model for the effect of temperature and water activity on the growth rate of *Vibrio parahaemolyticus*, *Int. J. Food Microbiol.*, *38*, 133–142.
Muhling, B. A., C. F. Gaitan, C. A. Stock, V. S. Saba, D. Tommasi, and K. W. Dixon (2017), Potential salinity and temperature futures for the Chesapeake Bay using a statistical downscaling spatial disaggregation framework, *Estuar. Coasts*, doi:10.1007/s12237-017-0280-8.
Najjar, R. G., et al. (2010), Potential climate-change impacts on the Chesapeake Bay, *Estuar. Coast. Shelf Sci.*, *86*, 1–20.
Newton, A., M. Kendall, D. J. Vugia, O. L. Henao, and B. E. Mahon (2012), Increasing rates of vibriosis in the United States, 1996-2010: Review of surveillance data from 2 systems, *Clin. Infect. Dis.*, *54*, S391–S395.
O'Neill, K. R., S. H. Jones, and D. J. Grimes (1992), Seasonal incidence of *Vibrio vulnificus* in the Great Bay estuary of New Hampshire and Maine, *Appl. Environ. Microbiol.*, *58*, 3257–3262.
Ortman, J. M., and C. E. Guarneri (2009), United States population projections: 2000 to 2050, *U. S. Census Bur.*, 1–19. [Available at http://www.census.gov/population/www/projections/analytical-document09.pdf.]
Parveen, S., K. A. Hettiarachchi, J. C. Bowers, J. L. Jones, M. L. Tamplin, R. McKay, W. Beatty, K. Brohawn, L. V. DaSilva, and A. DePaola (2008), Seasonal distribution of total and pathogenic *Vibrio parahaemolyticus* in Chesapeake Bay oysters and waters, *Int. J. Food Microbiol.*, *128*, 354–361.
Pascual, M., X. Rodó, S. P. Ellner, R. Colwell, and M. J. Bouma (2000), Cholera dynamics and El Niño-southern oscillation, *Science*, *289*, 1766–1769.
Payne, M. R., et al. (2015), Uncertainties in projecting climate-change impacts in marine ecosystems, *ICES J. Mar. Sci.*, *73*, 1272–1282.
Paz, S., N. Bisharat, E. Paz, O. Kidar, and D. Cohen (2007), Climate change and the emergence of *Vibrio vulnificus* disease in Israel, *Environ. Res.*, *103*, 390–396.
Pfeffer, C. S., M. F. Hite, and J. D. Oliver (2003), Ecology of *Vibrio vulnificus* in estuarine waters of eastern North Carolina, *Appl. Environ. Microbiol.*, *69*, 3526–3531.
Quinlan, J. R. (1992), Learning with continuous classes, *5th Australian Joint Conference on Artificial Intelligence, 92*, 343–348.
Quinlan, J. R. (1993), Combining instance-based and model-based learning, in *Proceedings of the Tenth International Conference on Machine Learning*, pp. 236–243.
R Core Team (2015), *R: A Language and Environment for Statistical Computing*, R Foundation for Statistical Computing URL, Vienna. [Available at http://www.R-project.org/.]
Ralston, E. P., H. Kite-Powell, and A. Beet (2011), An estimate of the cost of acute health effects from food- and water-borne marine pathogens and toxins in the USA, *J. Water Health*, *9*, 680–694.
Randa, M. A., M. F. Polz, and E. Lim (2004), Effects of temperature and salinity on *Vibrio vulnificus* population dynamics as assessed by quantitative PCR, *Appl. Environ. Microbiol.*, *70*, 5469–5476.
Rawlings, T. K., G. M. Ruiz, and R. R. Colwell (2007), Association of *Vibrio cholerae* O1 El Tor and O139 Bengal with the copepods *Acartia tonsa* and *Eurytemora affinis*, *Appl. Environ. Microbiol.*, *73*, 7926–7933.
Riahi, K., S. Rao, V. Krey, C. H. Cho, V. Chirkov, G. Fischer, G. Kindermann, N. Nakicenovic, and P. Rafaj (2011), RCP 8.5—A scenario of comparatively high greenhouse gas emissions, *Clim. Change*, *109*, 33–57.
Rodó, X., M. Pascual, G. Fuchs, and A. S. G. Faruque (2002), ENSO and cholera: A nonstationary link related to climate change, *Proc. Natl. Acad. Sci. U.S.A.*, *99*, 12901–12906.
Rothschild, B. J., J. S. Ault, P. Goulletquer, and M. Heral (1994), Decline of the Chesapeake Bay oyster population: A century of habitat destruction and overfishing, *Mar. Ecol. Prog. Ser.*, *111*, 29–39.

Scallan, E. R., M. Hoekstra, F. J. Angulo, R. V. Tauxe, M.-A. Widdowson, S. L. Roy, J. L. Jones, and P. M. Griffin (2011), Foodborne illness acquired in the United States—Major pathogens, *Emerg. Infect. Dis.*, *17*, 7–15.

Sedas, V. T. P. (2007), Influence of environmental factors on the presence of *Vibrio cholerae* in the marine environment: A climate link, *J. Infect. Dev. Ctries.*, *1*, 224–241.

Singleton, F. L., R. Attwell, S. Jangi, and R. R. Colwell (1982a), Effects of temperature and salinity on *Vibrio cholerae* growth, *Appl. Environ. Microbiol.*, *44*, 1047–1058.

Singleton, F. L., R. W. Attwell, M. S. Jangi, and R. R. Colwell (1982b), Influence of salinity and organic nutrient concentration on survival and growth of *Vibrio cholerae* in aquatic microcosms, *Appl. Environ. Microbiol.*, *43*, 1080–1085.

Tirado, M. C., R. Clarke, L. A. Jaykus, A. McQuatters-Gollop, and J. M. Frank (2010), Climate change and food safety: A review, *Food Res. Int.*, *43*, 1745–1765.

Turner, J. W., L. Malayil, D. Guadagnoli, D. Cole, and E. K. Lipp (2014), Detection of *Vibrio parahaemolyticus*, *Vibrio vulnificus* and *Vibrio cholerae* with respect to seasonal fluctuations in temperature and plankton abundance, *Environ. Microbiol.*, *16*, 1019–1028.

Urquhart, E. A., B. F. Zaitchik, D. W. Waugh, S. D. Guikema, and C. E. Del Castillo (2014), Uncertainty in model predictions of *Vibrio vulnificus* response to climate variability and change: A Chesapeake Bay case study, *PLoS One*, *9*, e98256.

United States Food and Drug Administration (2005), Quantitative risk assessment on the public health impact of pathogenic *Vibrio parahaemolyticus* in raw oysters. Center for Food Safety and Applied Nutrition. [Available at http://www.fda.gov/Food/FoodScienceResearch/RiskSafetyAssessment/ucm050421.htm.]

Virginia Department of Health (2016), *Vibrio* control plan, 11 pp.

Vezzulli, L., M. Previati, C. Pruzzo, A. Marchese, D. G. Bourne, and C. Cerrano (2010a), *Vibrio* infections triggering mass mortality events in a warming Mediterranean Sea, *Environ. Microbiol.*, *12*, 2007–2019.

Vezzulli, L., C. Pruzzo, A. Huq, and R. R. Colwell (2010b), Environmental reservoirs of *Vibrio cholerae* and their role in cholera, *Environ. Microbiol. Rep.*, *2*, 27–33.

Vezzulli, L., R. R. Colwell, and C. Pruzzo (2013), Ocean warming and spread of pathogenic *Vibrios* in the aquatic environment, *Microb. Ecol.*, *65*, 817–825.

Vezzulli, L., C. Grande, P. C. Reid, P. Hélaouët, M. Edwards, M. G. Höfle, M. G. Brettar, R. R. Colwell, and C. Pruzzo (2016), Climate influence on *Vibrio* and associated human diseases during the past half-century in the coastal North Atlantic, *Proc. Natl. Acad. Sci. U.S.A.*, *113*, E5062–E5071, doi:10.1073/pnas.1609157113.

Vrac, M., M. L. Stein, K. Hayhoe, and X.-Z. Liang (2007), A general method for validating statistical downscaling methods under future climate change, *Geophys. Res. Lett.*, *34*, L18701, doi:10.1029/2007GL030295.

Waldman, R. J., E. D. Mintz, and H. E. Papowitz (2013), The cure for cholera—Improving access to safe water and sanitation, *N. Engl. J. Med.*, *368*, 592–594.

Weis, K. E., R. M. Hammond, R. Hutchinson, and C. G. M. Blackmore (2011), *Vibrio* illness in Florida, 1998–2007, *Epidemiol. Infect.*, *139*, 591–598.

World Health Organization (2016), Cholera: Fact sheet. [Available at www.who.int/mediacentre/factsheets/fs107/en/, Accessed November 11th, 2016.]

Wood, S. (2006), *Generalized Additive Models: An Introduction With R*, CRC Press, Boca Raton, Fla.

Wright, A. C., R. T. Hill, J. A. Johnson, M. C. Roghman, R. R. Colwell, and J. G. Morris (1996), Distribution of *Vibrio vulnificus* in the Chesapeake Bay, *Appl. Environ. Microbiol.*, *62*, 717–724.

Yukimoto, S., et al. (2012), A new global climate model of the Meteorological Research Institute: MRI-CGCM3—Model description and basic performance, *J. Meteor. Soc. Jpn.*, *90A*, 23–64.

Züur, A., E. Ieno, N. Walker, A. Saveliev, and G. Smith (2009), *Mixed Effects Models and Extensions in Ecology With R*, *Statistics for Biology and Health*, 574 pp., Springer New York.